Reed as a gasification fuel: a comparison with woody fuels

S. Link[1], Ü. Kask[1], A. Paist[1], A. Siirde[1], S. Arvelakis[2], M. Hupa[3], P. Yrjas[3] and I. Külaots[4]

[1]Department of Thermal Engineering, Tallinn University of Technology, Estonia
[2]Department of Chemical Engineering, National Technical University of Athens, Greece
[3]Åbo Akademi Process Chemistry Centre, c/o Combustion and Materials Chemistry, Finland
[4]Division of Engineering, Brown University, Providence, RI, USA

SUMMARY

Reed and coniferous wood can be used for energy production *via* thermochemical conversion, for instance by gasification. The rate-determining step of the gasification process is the reaction between the char and the gaseous environment in the gasifier, whose rate depends on variables such as pressure, temperature, particle size, mineral matter content, porosity, *etc*. It is known that reactivity can be improved by increasing the temperature, but on the other hand the temperature achieved in the reactor is limited due to the ash fusion characteristics. Usually, the availability of reed as a fuel is locally modest and, therefore, it must be blended with other fuels such as wood. Blending of fuels brings together several problems relating to ash behaviour, i.e. ash fusion issues. Because there is no correlation between the ash fusion characteristics of biomass blends and their individual components, it is essential to carry out prior laboratory-scale ash fusion tests on the blends. This study compares the reactivity of reed and coniferous wood, and the ash fusion characteristics of blends of reed and coniferous wood ashes. When compared with Douglas fir and reed chars, pine pellets have the highest reactivity. Reed char exhibits the lowest reactivity and, therefore, it is advantageous to gasify reed alone at higher gasification temperatures because the ash fusion temperatures of reed are higher than those of woody fuels. The ash produced by reed and wood blends can melt at lower temperatures than ash from both reed and wood gasified separately. Due to this circumstance the gasification temperature should be chosen carefully when gasification of blends is carried out.

KEY WORDS: ash fusion; biomass blends; co-gasification; reactivity

INTRODUCTION

Fuels for biomass energy production

Reed (*Phragmites australis*) is widespread, both onshore and offshore, in the coastal areas of Estonia and southern Finland, and the species is well known all over the world. Reed has encroached gradually upon the coastline and its expansion has been accelerated by human activities such as the cessation of coastal meadow management, eutrophication and climate change. Reed has been used as a source of energy in various European countries including Estonia, Romania, Hungary, Finland and The Netherlands (Ikonen & Hagelberg 2007).

The potential of reed for energy production is regarded as modest (e.g. only 292 GWh/year in Estonia) relative to that of other types of biomass such as wood. Douglas fir has been widely planted for 30 years in Europe, especially in France and Germany, and is now an emerging source of saw logs, thinning logs, top logs and sawmill chips. The expected annual harvest of Douglas fir in France is around 6 million m^3 by the year 2015 (Chantre *et al*. 2002). In Europe, as well as around the world, the production of wood pellets amounts to tens of millions of tonnes per year (Ljungblom 2009).

Gasification process and ash behaviour

The char conversion that follows pyrolysis in the gasification process is generally much slower than pyrolysis itself and is, therefore, the rate-determining step (Cetin *et al*. 2005). High char reactivity is needed to obtain higher energy outputs from the reactors (Zanzi *et al*. 1996).

The gasification temperature is an important factor affecting reactivity, ash fusion characteristics, tar cracking etc. On the other hand, the ash fusion temperature (mainly) determines the maximum temperature in the reactor, as ash fusion or agglomeration in fluidised bed reactors should be avoided. The properties of the ash from a fuel mix cannot be predicted from the known characteristics of the ash formed by each fuel individually. The interaction between the ashes from different fuels is poorly understood and a number of unexpected outcomes have been reported when fuel mixtures

have been used (Vamvuka *et al*. 2009). Blending fuels without sufficient prior investigation and analysis can easily exacerbate problems such as slagging, fouling and corrosion. Moreover, the behaviour of inorganic constituents, and of some organic constituents, is not necessarily linearly additive for blends. Therefore, surprises—some favourable and many unfavourable—may occur (Tillman *et al*. 2012, Hupa 2012).

Aim of the study

In this study we investigated the oxidation reactivity of chars derived by pyrolysis of reed, pine pellets and Douglas fir wood chips, and the ash fusion characteristics of reed and coniferous wood residue blends, with focus on co-gasification issues.

METHODS

Choice and characterisation of materials

The samples selected for the investigation of char reactivity were: pelagian reed from the west coast shorelines and islands of Estonia, and commercial pine pellets and Douglas fir wood chips originating from the vicinity of Munich in Germany. To characterise the ash fusion of blends, the pelagian reed was used with coniferous wood residue from an industrial sawmill near Tallinn (in Estonia).

The reed, Douglas fir wood chip and pine pellet samples for characterisation of char reactivity (hereafter referred to as R1, DF and PP), as well as their char samples (R800, DF800 and PP800), were analysed and characterised on the basis of proximate and ultimate composition analyses and ash chemical analysis in accordance with American Society for Testing and Materials (ASTM) methods such as D 1102-84, D 3175-89a, D 5142-90, D5373-93 and D 4208-88. In all cases, the oxidation for ash chemical analysis was performed at a temperature of 600 °C.

The reed and coniferous wood residue samples for ash fusion characterisation (hereafter referred to as R2 and CW) were analysed in accordance with the standard methods in CEN/TS 14774-1:2004, CEN/TS 14775:2004 and CEN/TS 15148:2005 for proximate analysis. Ultimate composition was determined with a Vario EL CHNOS elementary analyser, and chemical analysis of ash was carried out in accordance with the standard methods in DIN 51729 and ISO 334:1992.

Because of the relatively low char yield of pine pellets in the pyrolysis experiments, the proximate analysis of pine pellet char was performed using a SDT Q600 thermogravimetric analyser (TGA). In the TGA experiments, each sample was first heated at 20 °C min^{-1} from ambient temperature to 105 °C in a nitrogen gas flow of 90 mL min^{-1} to determine the moisture content. Then, the temperature was increased at a rate of 50 °C min^{-1} to 900 °C, where it was held for 7 minutes to determine the sample's volatile content. After this, the temperature was lowered to 600 °C over 20 minutes, then the 100 mL min^{-1} air flow was led into the analyser to determine the ash content after burning of the sample.

The ash fusion characteristics were determined according to the standard method of CEN/TS 15370-1:2006. The shrinkage temperature (ST), deformation temperature (DT), hemispherical temperature (HT) and flow temperature (FT) were evaluated.

Pyrolysis

An atmospheric fixed-bed reactor was used to prepare the char samples. The R, PP and DF parent samples were heated at a rate of 20 °C min^{-1} to 800 °C and held isothermally for 15 minutes before cooling to ambient temperature. The methodology, together with a detailed description of the system, has been reported elsewhere (Link *et al*. 2008). Nitrogen (flow rate 1 L min^{-1}) was used as the carrier gas in all pyrolysis experiments.

Surface area and porosity

Surface area, porosity, pore size distribution *etc*. are important factors affecting the rate of the reaction between char and gas.

Nitrogen adsorption isotherms at -196 °C and carbon dioxide isotherms at 0 °C were obtained from all of the char samples by a volumetric technique using a Quantachrome Autosorb-1 instrument. Prior to surface area analysis, all of the char samples were outgassed at 280 °C overnight under vacuum to ensure complete removal of surface contaminants. Because of the pressure limitation of the instrument, the maximum partial pressure (P/P0) of 0.03 was attained when CO_2 isotherms at 0 °C were recorded (PCO_2 sat = 3484.8 kPa at 0 °C). The adsorption uptake data at partial pressures of N_2 from 10^{-6} to 1 were requested in order to obtain full N_2 isotherms. The specific Brunauer-Emmett-Teller (BET) surface areas from the N_2 isotherms of the char samples were determined over the partial pressure (P/P0) range where the BET equation had the highest correlation coefficient (at least 0.99) (Brunauer *et al*. 1938, Gregg & Sing 1982). For most non-microporous samples, the commonly accepted range of P/P0 for the BET equation is 0.05 to 0.3 (N_2 isotherms). However, because of the highly microporous nature of the char samples, the relative pressure range of the isotherms for BET surface area determination

required adjustment. Therefore, in this work, the BET surface areas were defined at significantly lower relative pressure (P/P0) values, down to 0.01–0.05.

The porosity values presented here were calculated using the N_2 adsorption isotherms of the char samples. The microporosity of the char samples was determined using the Dubinin-Radushkevich (DR) model (Gregg & Sing 1982). Their mesoporosity was determined by subtracting the DR microporosity value from the total porosity at an isothermal relative pressure of P/P0=0.95, and their macroporosity was calculated by subtracting the total porosity at relative pressure P/P0=0.95 from the porosity value at relative pressure P/P0=0.99.

The pore size distributions (PSDs) of the char samples were determined from the N_2 adsorption isotherms at -196 °C and the CO_2 adsorption isotherms at 0 °C using density functional theory (DFT) (Lastoskie *et al*. 1993, Lozano-Castello *et al*. 2004). The PSDs are reported according to the classification of the International Union of Pure and Applied Chemistry (IUPAC), which defines micropores as pores smaller than 20 Å, mesopores as pores in the range 20–500 Å, and macropores as pores larger than 500 Å.

Char reactivity measurement

A Deutsche Montan Technologie (DMT) high-pressure thermogravimetric apparatus (HPTGA) operating at atmospheric pressure was used for the char reactivity tests. The sample was initially held in the reactor under helium (He) gas flow. Then, the desired reaction temperature was selected, and the reactor was heated to the target temperature of 850 °C. After this temperature was attained, the sample holder was lowered into the preheated reactor. A steady sample mass was achieved in 150–300 s (Phase I), then the gasification agent CO_2 at a flow rate of 1 L min^{-1} was introduced to the reactor (Phase II). A detailed description of the system, which includes a schematic diagram, is given by Whitty *et al*. (1998).

Reactivity data analysis

A typical HPTGA mass loss curve is shown in Figure 1. M_0 represents the initial mass of the char, M(t) is the mass of the char at time t, and M_f is the mass of the residue.

Various definitions may be used to determine reactivity (Barrio *et al*. 2001). In this work, we present reactivity in terms of the char gasification rate as a function of char conversion. The char

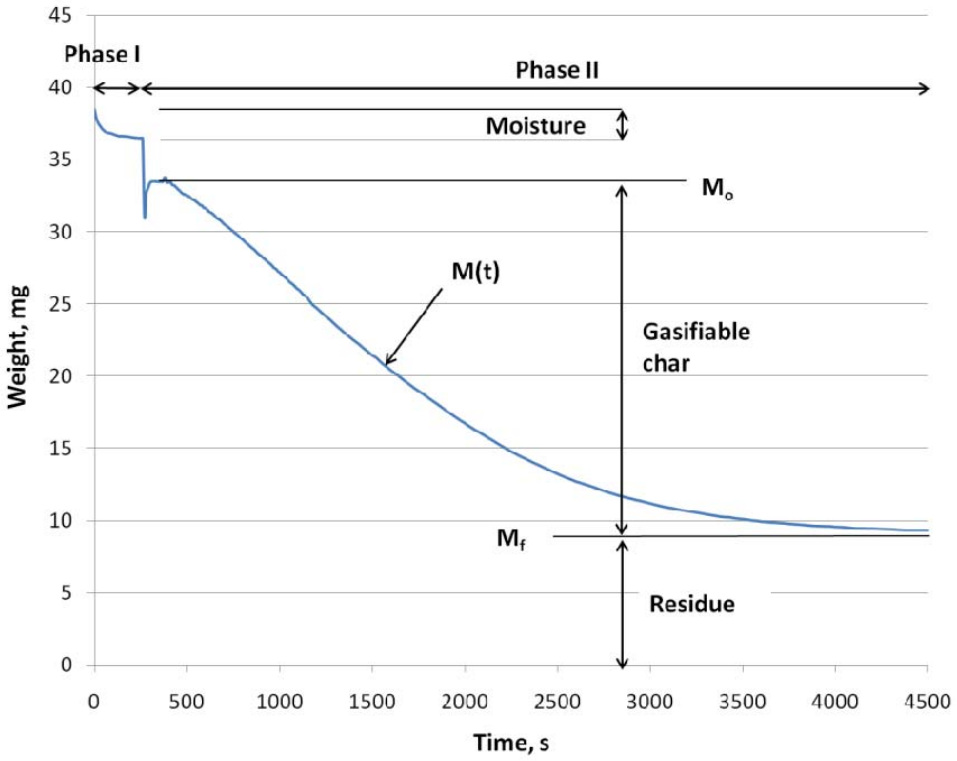

Figure 1. A typical weight loss curve observed during a HPTGA (high-pressure thermogravimetric apparatus) determination of char reactivity. M_0 is the initial mass of char, M(t) is the mass of char at time t, and M_f is the mass of the residue.

gasification rate in units of min^{-1} at any particular conversion value is defined as:

$$r = \frac{dX}{dt} \quad [1]$$

where r is the reaction rate and

$$X = \frac{M_0 - M(t)}{M_0 - M_f} \quad [2]$$

RESULTS

Material characterisation

The PP material had a relatively low ash content of 0.2 % on a dry weight basis, and the ash contained (mainly) 37.3 weight percent (wt%) calcium oxide, which corresponds to 0.08 wt% in parent fuel (see also Tables 1 and 2). The DF had the highest ash content (6.7 wt% on a dry basis) and the highest potassium oxide content in parent fuel (0.3 wt%). The ash content of the reed (R1) was 3.2 wt% (dry basis), and the ash consisted mainly of silica

Table 1. Results of analysis and characterisation of the biomass samples. n.d. = not determined.

	Proximate analysis, dry basis (wt%)				Ultimate analysis, dry basis (wt%)					
	Moisture	Ash	Volatile matter	Fixed carbon	N	C	H	S	Cl	O
R1	5.4	3.2	80.3	16.5	0.4	47.4	5.7	0.2	n.d.	43.1
DF	7.7	6.7	72.3	21.0	0.6	48.5	4.9	0.05	n.d.	39.3
PP	5.9	0.2	83.3	16.5	0.3	50.5	5.9	0.2	n.d.	43.0
R800	6.9	16.0	6.7	77.3	1.7	59.2	1.2	n.d.	n.d.	21.9
DF800	6.5	20.8	9.5	69.7	1.5	56.7	0.9	n.d.	n.d.	20.1
PP800	8.6	4.1	7.1	88.8	1.0	64.1	1.2	n.d.	n.d.	30.6
R2	5.4	3.5	82.1	14.4	0.3	47.1	7.4	0.02	0.04	41.7
CW	32.3	0.6	83.5	15.9	0.3	50.0	5.9	0.02	0.01	42.7

Table 2. Results of chemical analyses of ash of the biomass samples (parent fuels R1, R2, DF, PP and CW and char samples R800, DF800), expressed as oxides, wt%. The PP800 char sample is omitted because the relatively low ash content of the pine pellets (Table 1) meant that it was not possible to generate sufficient PP800 ash for chemical analysis within a reasonable number of pyrolysis experiments. n.d. = not determined.

	R1	DF	PP	R800	DF800	R2	CW
K_2O	5.9	4.1	7.7	3.3	4.7	2.5	20.4
Na_2O	8.4	1.5	1.3	2.8	1.4	2.4	0.3
CaO	2.9	10.9	37.3	4.1	9.6	4.5	41.5
MgO	1.4	4.9	9.1	1.5	7.7	2.2	12.9
SiO_2	73.7	55.5	11.2	83.4	51.9	81.9	1.1
Al_2O_3	0	11.6	5.0	0.9	13.7	1.1	2.2
Fe_2O_3	1.1	7.2	4.8	1.4	6.6	0.4	0.16
SO_3^-	n.d.	n.d.	n.d.	n.d.	n.d.	2.0	3.2
Cl^-	0.6	0.7	1.0	0.2	0.4	0.6	0.1

(73.7 wt%), which corresponds to 2.4 wt% of the parent material and is lower than the 3.7 wt% for the DF sample.

The O/C and H/C ratios of the char samples (molar basis) are shown in Table 3. PP800 had the highest O/C ratio. R800 had the highest H/C ratio, but the value for PP800 was only moderately lower.

Table 3. O/C and H/C ratios of char samples, on molar basis.

	O/C	H/C
R800	0.28	0.25
DF800	0.27	0.19
PP800	0.35	0.22

Specific surface area and porosity

The N_2- and CO_2-specific BET surface areas of all chars tested are quite comparable (Table 4). The N_2-specific BET surface areas range from 316 to 485 m^2 g^{-1}. The CO_2-specific BET surface areas range from 398 to 536 m^2 g^{-1}, and are slightly lower than the CO_2 specific DR (Dubinin-Radushkevich) surface areas (545–736 m^2 g^{-1}). The specific surface area is clearly higher for the PP800 char sample than for the other chars studied.

Table 4. Specific surface areas (m^2 g^{-1}).

	BET N_2	BET CO_2	DR CO_2
R800	357	435	583
DF800	316	398	545
PP800	485	536	736

The porosity values in Table 5 show that the reed and woody fuel chars are mostly microporous, with 70–80 % of their pore volumes accounted for by micropores (below 20 Å) and only about 15 % accounted for by mesopores (20–500 Å). These results also show that the DR (CO_2) microporosity is slightly higher than the DR (N_2) microporosity.

The results of DFT PSD analysis for R800, DF800 and PP800 are shown in Figures 2 and 3. All of the PSDs are clearly quite similar and, therefore, completely independent of char origin.

The CO_2 DFT PSD analysis also shows that the super-micropores (smaller than 8 Å) in these chars are not available in the N_2 DFT analysis plot (Figure 2). It seems quite evident that both adsorbates, N_2 and CO_2, are needed when adsorption characteristics of carbonaceous samples with significant microporosity are investigated (Lozano-Castello *et al*. 2004, Della Rocca *et al*. 1999).

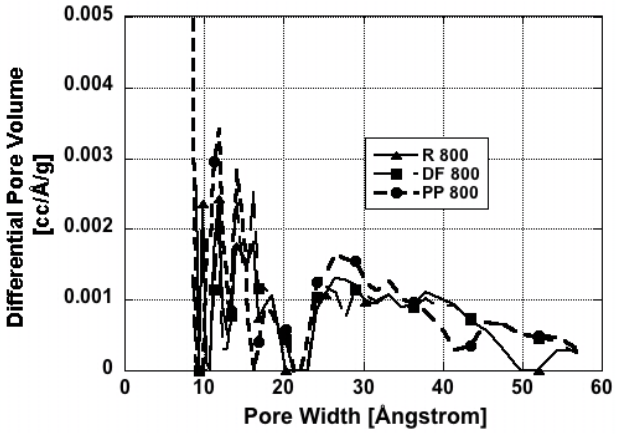

Figure 2. DFT/Monte-Carlo differential pore volume distribution. DFT Kernel used: N_2 at -196 °C on carbon.

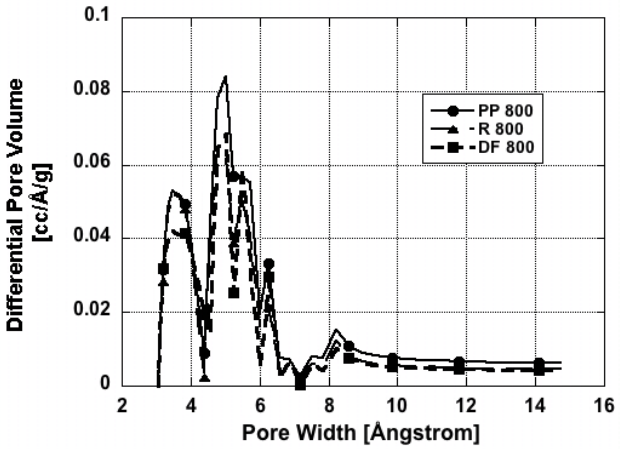

Figure 3. DFT/Monte-Carlo differential pore volume distribution. DFT Kernel used: CO_2 at 0 °C on carbon.

Table 5. Porosities obtained from N_2 and CO_2 isotherms (mL g^{-1}).

	DR (CO_2) Microporosity	DR (N_2) Microporosity	(N_2) Mesoporosity	(N_2) Macroporosity	(N_2) Total porosity
R800	0.203	0.137	0.033	0.031	0.200
DF800	0.190	0.121	0.039	0.017	0.176
PP800	0.257	0.184	0.038	0.010	0.231

Char reactivity

The char reactivity measurements were performed at 850 °C. The weight signal curve shifts downward at the end of Phase I (see also Figure 1), and the increase in sample weight at the beginning of Phase II was probably due to a buoyancy effect resulting from the change in the reactor feed gas.

The reaction rates *versus* char conversion of the R800, DF800 and PP800 samples are shown in Figure 4. The reaction rate of R800 was constant until the conversion rate reached 40 %, after which it declined. The reaction rate of DF800 decreased until the conversion rate reached 40–50 %, then remained constant until the conversion rate was 60–70 %, after which it declined again. The reaction rate of PP800 was constant until the conversion rate reached 60–70 %, then decreased.

Conversion rates *versus* time for the gasification tests are shown in Figure 5. PP800 exhibited the shortest gasification time and R800 the longest. The results of this analysis place the reactivity rates of the samples in the same order as discussed above.

Ash fusion characteristics

The series of tests for the ash fusion characteristics of wood (CW) and reed (R2) ash blends were carried out over a range of different proportions. The proportion of wood ash varied from 10 % to 90 %. The results are presented in Table 6. The proportions of parent fuels in the blends were calculated according to the ash contents of the reed (R2) and wood (CW) samples.

Figure 6 shows the ash fusion temperatures plotted against the proportions of both wood ash and parent wood material in the wood-reed blends that were tested.

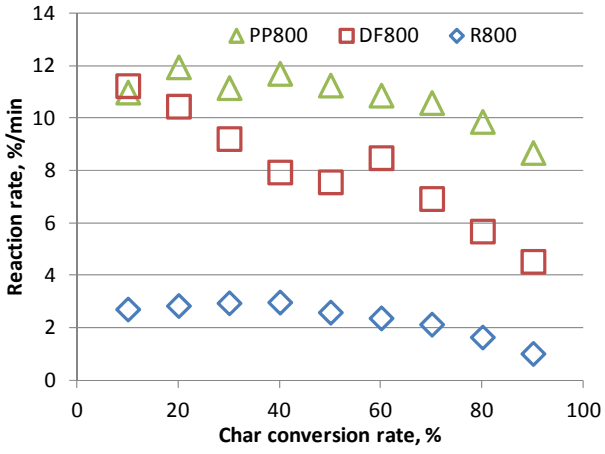

Figure 4. Reactivity of the char samples during the course of gasification at 850 °C.

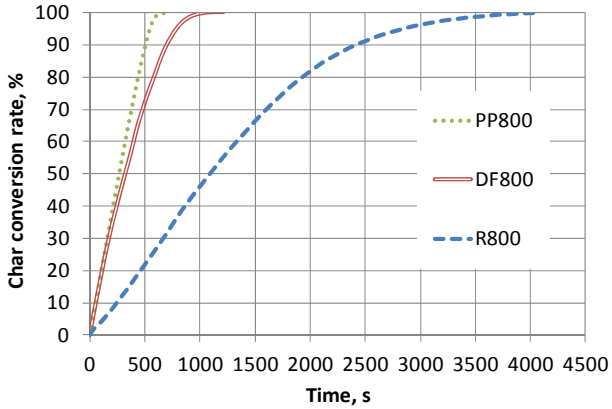

Figure 5. Conversion rate *versus* time for the char sample gasification tests at 850 °C.

DISCUSSION

Reactivity

Gasification rates are influenced by a number of process variables, such as particle size and size distribution, char porosity and pretreatment, mineral content of char, and temperature and partial pressures of the gasifying agents (Liliedahl & Sjöström 1997). In this study the pyrolysis conditions, gasification conditions, particle size and size distribution were the same for all samples. Hence, the differences in reactivity of the chars are due to differences in their chemical and physical properties only.

Several studies have focused on the influence of wood type on the CO_2 gasification process. In general, the differences in reactivity amongst the fuels can be explained in terms of their mineral matter content, composition and catalytic properties (Barrio *et al*. 2001). The presence of inorganic constituents in chars plays an important role in oxidation kinetics because of their catalytic effects. Na, K, and Ca, which are commonly present in biomass, show significant activity as gasification catalysts (Figueiredo & Moulijn 1986, Jüntgen 1983, Wood & Sancier 1984). It has been shown that alkali metals are approximately ten times more active in catalysing char gasification than alkali earth metals (Risnes *et al*. 2001). Kannan & Richards (1990) found that the catalytic effect of K was reduced by its reaction with silica to form silicate during pyrolysis, but catalysis of gasification by Ca does not appear to be significantly reduced by the presence of silica. The CO_2 gasification rate depends upon the silicon content of the parent fuel and, when the silicon content is low, also on the sum of its K and Ca contents. The dependency of gasification rate upon the silicon content of the

Table 6. Fusion characteristics of ash from different blends of wood (CW) and reed (R2). ST: shrinkage temperature; DT: deformation temperature; HT: hemispherical temperature; FT: flow temperature; units: °C.

		Wood ash/reed ash, % (dry weight)								
		Wood	90/10	80/20	70/30	50/50	40/60	30/70	20/80	10/90	Reed
			Wood parent material/reed parent material, % (dry weight)								
			98/2	96/4	93/7	85/15	80/20	71/29	59/41	39/61	
1st test series	ST	1090	1050	1050	1030	995	1000	1000	1055	1225	1330
	DT	1110	1090	1070	1045	1030	1070	1035	1150	1255	1360
	HT	1170	1105	1090	1080	1100	1120	1125	1240	1310	1410
	FT	1190	1125	1100	1110	1120	1145	1180	1290	1355	1460
2nd test series	ST	1085	1040	1035	1020	1000	970	995	1040	1230	1335
	DT	1120	1080	1055	1040	1035	1025	1020	1090	1260	1360
	HT	1170	1100	1080	1080	1095	1095	1120	1225	1315	1420
	FT	1200	1120	1100	1115	1125	1135	1170	1290	1365	1450
Average	ST	1088	1045	1043	1025	998	985	998	1048	1228	1336
	DT	1115	1085	1063	1043	1033	1048	1028	1120	1258	1360
	HT	1170	1103	1085	1080	1098	1108	1123	1233	1313	1415
	FT	1195	1123	1100	1113	1123	1140	1175	1290	1360	1455

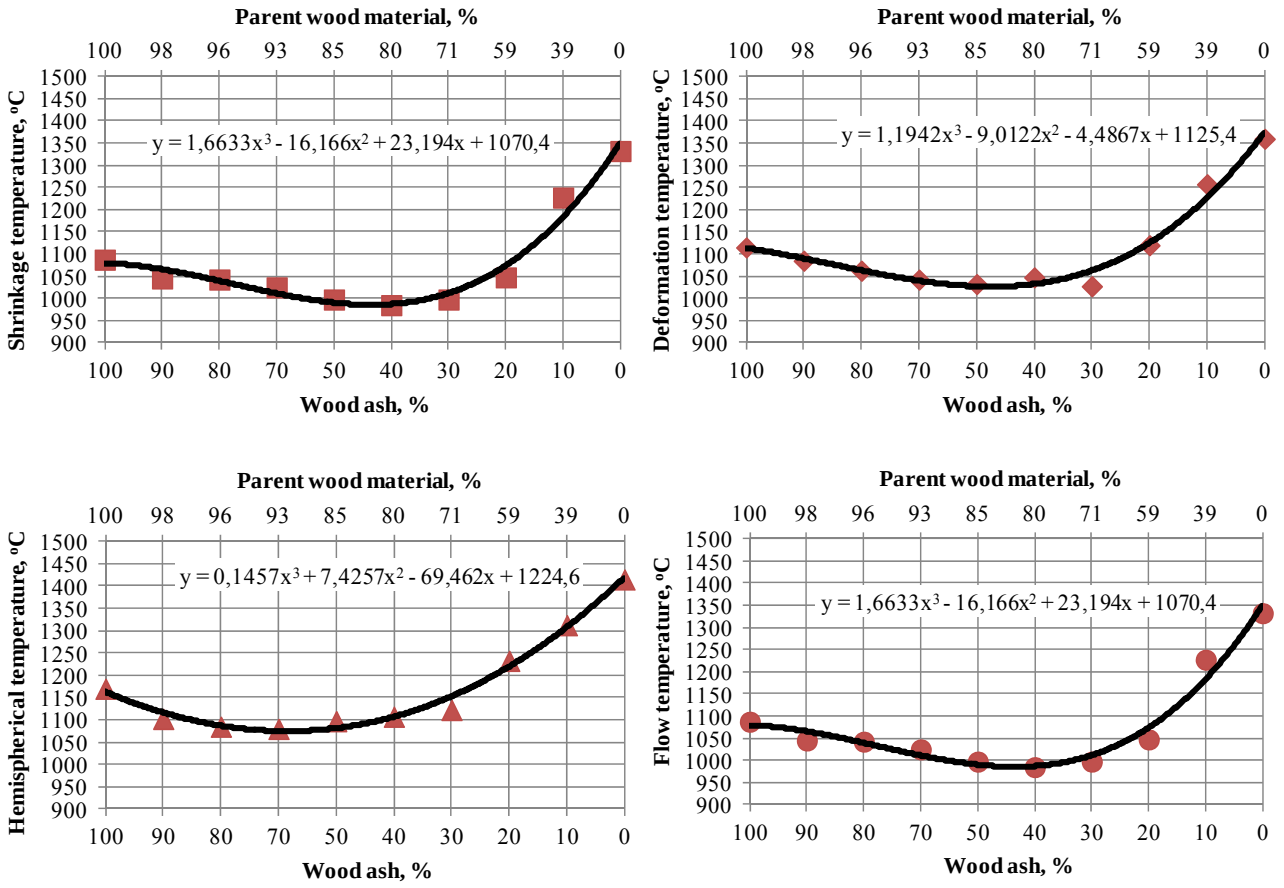

Figure 6. Plots of ash fusion temperature data for blends of wood and reed (see also Table 6).

parent fuel was also discussed by Moilanen (2006). Experimental and theoretical studies by Sørensen *et al*. (2000) have shown that the reactivity of char is dependent upon the silicon as well as the potassium content and the form of the potassium compound. Thus, according to the literature, the catalytic effect of mineral matter content on biomass char reactivity is mainly related to alkali/alkali earth metals *versus* silicon content.

It was evident that the wood chars exhibited higher reactivity than the reed char. In Figures 4 and 5, the order of reactivity of the chars can be seen as: PP800>DF800>>R800. At conversion rates of 20–40 %, the reaction rate of PP800 was up to four times that of R800. The reaction rate of DF800 was around three times that of R800.

The R800 and DF800 samples had higher ash contents than the PP800 char sample, as well as higher alkali/alkali earth metal, chlorine, and silicon contents.

The interaction between the compounds present in mineral matter can inhibit the catalytic effect of the alkali/alkali earth metals, leading to a situation in which, for instance, potassium is totally inactive (Van Heek & Mühlen 1985). The catalytic deactivation reaction depends only upon time and is not much influenced by temperature and pressure. At high conversion, the catalyst seems to lose its contact with carbon and, consequently, its activity (Moilanen & Mühlen 1996). The process of catalyst deactivation is already taking place during the pyrolysis step, which in our study was so-called slow pyrolysis, and continues during the gasification step. From the work of Zevenhoven-Onderwater *et al*. (2001), we infer that the following processes were involved:

(1) formation of calcium, potassium, magnesium, sodium and aluminium silicates during thermal treatment;
(2) the high silica content of reed and Douglas fir chars yielded potassium silicates, whereas high silica and chlorine contents favoured potassium silicate formation combined with the release of HCl and the formation of K_2CO_3 did not occur;
(3) in the case of the pine pellets (with low silica content), K_2CO_3, which is known to be a better catalyst than, for instance, sodium and calcium carbonates (Sutton *et al*. 2001), was formed during gasification, probably along with KCl.

The formation of silicates reduces the amount of available alkali and alkaline earth metals taking part in the solid-gas reaction on active sites. According to Radović *et al*. (1983), the reactivity is dependent upon carbon active sites rather than total surface area. Van Heek & Mühlen (1985) have concluded that the extension of total surface area alone could not be the dominating factor, which is more likely to be qualities of the surface (such as activity and accessibility) which provide possibilities for blockage of areas by minerals. Bar-Ziv & Kantorovich (2001) concluded that the evolution of reactivity during conversion is influenced by changes in the porous structure, and coalescence of microcrystals can be used to represent the change in concentration of the reactive sites. Livneh *et al*. (2000) confirmed that the most significant change in reactivity occurs in the range 0–30 % conversion, and the lower reactivity at conversion rates above 55 % can be explained by the consumption of small microcrystals, which are generally more reactive than large ones.

In the case of R800 and DF800, the initial increase in the reaction rate could be associated with an increase in surface area as well as active sites during the early stages of gasification. In terms of porosity, the peak in the reaction rate is thought to arise from two opposing effects, namely the increase in reactive surface area as the micropores grow and its decline as the pores collapse progressively at their intersections (coalescence) (Struis *et al*. 2002). A decline in the reaction rate is associated with the deactivation of catalysts and, therefore, the participation of fewer active sites in the reaction between char and gaseous environment.

The lower reactivity of R800 compared to that of DF800 may arise from the 20 % higher Si and 3 times lower alkali, alkali earth, and iron contents of the char sample, which could enhance the interaction between the mineral matter compounds, tending to inhibit the catalysts and active sites available for the solid-gas reaction.

Our results indicate that PP800 is more reactive than R800 and DF800 despite the fact that, in comparison with the pine pellets, reed has more than five times and Douglas Fir more than fifteen times the content of elements (K, Na, Ca, Mg and Fe) capable of acting as catalysts. The ash content of pine pellet char is 4 % and, according to chemical analysis of the ashed parent material, it contains mainly Ca and K and is not rich in silicon. Therefore, on the basis of the results, we reason that PP800 had the highest reactivity amongst the chars that we studied due to its higher porosity, its pore structure, its relatively high O/C ratio, and the nature of its mineral content. K and Ca did not form silicates but, rather, compounds bound to the carbon matrix that functioned as the active sites.

The steady reaction rate of PP800 throughout the gasification process indicates that pine pellet char particles have the so-called ‘thin plate’ shape, i.e. the length and width of the particle are an order of magnitude larger than its thickness, and the particle

surfaces are porous. One might imagine these plates piled one on top of another (Figure 7), so that the spaces between them would act as 'through' pores (with two open ends), as shown in Figure 8 (Leofanti *et al*. 1998). With this arrangement, the gasification agent could react with and consume the char material forming the 'plate' walls without significantly changing the total and active surface areas. However, the evolution of the total surface area of the studied chars during the gasification process needs further investigation.

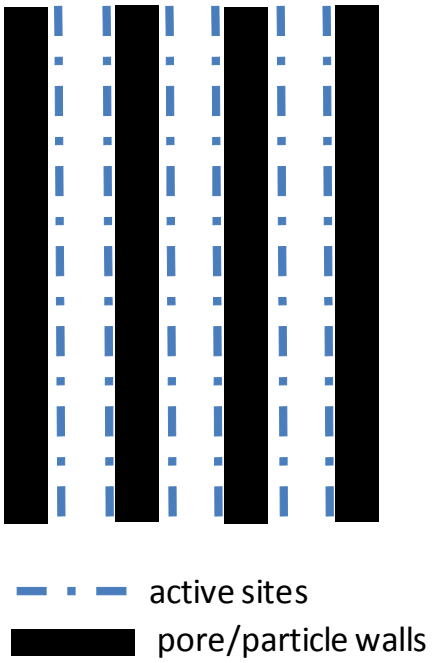

Figure 7. Visualisation of the pore structure of PP800.

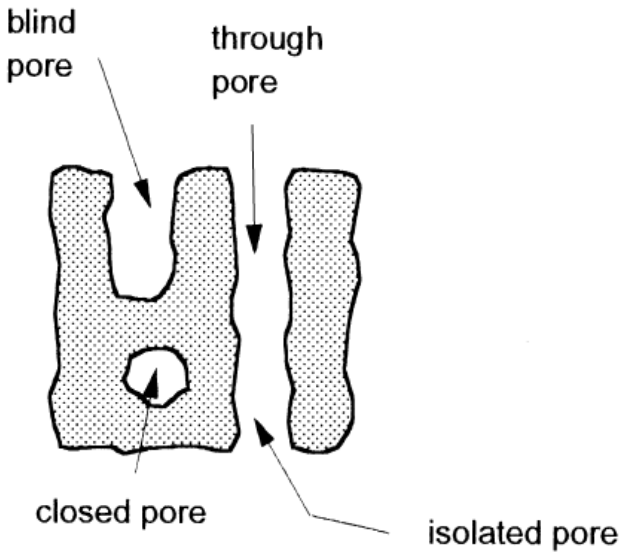

Figure 8. Different types of pores (Leofanti *et al*. 1998).

Ash fusion characterisation

Slagging, fouling and corrosion of surfaces are ash-related problems that should be examined when blends of fuels are used, since they can lead to reduced efficiency, capacity and availability of facilities, and thus increase the unit cost of the generated power. Therefore, a knowledge of how mixing different fuels affects the properties of the ash they produce can make it possible to avoid fuel combinations with unwanted properties, or even to design them to produce ash materials for particular applications (Vamvuka *et al*. 2009). In fluidised bed reactors, agglomeration causes defluidisation (Khan *et al*. 2009, Saidur *et al*. 2011). This can occur as a result of two phenomena, namely: (i) accumulation of low-melting-point salts of K and P, and (ii) in the presence of SiO_2 from sand and Ca from fuel, K_3PO_4 can react with SiO_2 to form low-melting-point K and Ca silicates, while the P binds with Ca.

The mineral matter content affects the reactivity of the chars as well as the behaviour of the fuel in the reactor in terms of slagging, fouling, corrosion, agglomeration, ash melting *etc*. According to Arrhenius' law, the higher the temperature the greater the reaction rate will be. But, on the other hand, increased temperature in the reactor could lead to the ash melting and consequent agglomeration problems.

For example, it can be seen from Figure 6 that the flow temperature of pure reed ash is 260 °C higher than that of pure wood ash, and the curves describe the temperature dependency of specific ash fusion characteristics on the proportions of reed and wood ash in the fuel blend. The proportions of wood ash corresponding to the minima of the trendline curves presented in Figure 6 were calculated using the Excel trendline function (third order polynomial equation). The minimum shrinkage temperature occurs at 46 % wood ash, corresponding to 83 % (dry basis) of parent wood fuel in the blend; the minimum deformation temperature at 51 % wood ash or 86 % parent wood; and the minimum hemispherical and flow temperatures at 66 % wood ash or 92 % parent wood. From the range of fusion characteristics shown in Figure 6 it can be seen that, in general, the minimum temperatures at which fusion of ash from wood and reed blends occurs are roughly 100 °C lower than the equivalent fusion temperatures for pure wood ash.

On the other hand, the shapes of the characteristic curves mean that the fusion temperatures for pure wood ash are comparable to those for a blend of ~20 % wood ash with ~80 % reed ash, which corresponds to a parent fuel blend of ~60 % wood with ~40 % reed (dry weight basis).

The standardised procedure for ash fusion

characterisation applied in this study is considered to be of only average value for biomass. Many other non-standard methods are available, such as viscosity measurements (Arvelakis *et al*. 2006, Arvelakis & Frandsen 2007) and TGA/DCS (thermogravimetric analysis/differential scanning calorimetry), also known as simultaneous thermal analysis (STA) (Arvelakis *et al*. 2004, Hansen *et al*. 1999). Future work will focus on characterising the ash blends studied here using such non-standard methods, as well as on the melting behaviour of the ash remaining after co-gasification of different biomass fuels including reed and reed-wood blends, in a commercial or non-laboratory scale gasifier.

CONCLUSIONS

1. Wood chars (derived from pine pellets and Douglas fir) are more reactive CO_2 gasification fuels than reed char produced under the same conditions. The time required for 100 % conversion is longest for reed char and shortest for pine pellet char under the same gasification conditions, indicating that pine pellet is the most reactive of the fuel types studied.
2. The high reactivity of pine pellets means that they could produce the same energy output as Douglas fir and/or reed from a smaller reactor producing less ash and, therefore, incurring lower landfill costs.
3. The differences in reactivity between fuels can be explained by differences in mineral matter content, pore structure, internal surface area and active sites. For gasification at similar temperatures, the results of this study indicate that a combination of favourable char structure and low Si content (pine pellet) is a better fuel characteristic than high alkali/alkali earth metal content (Douglas fir wood chip) if accompanied by high Si content (Douglas fir and reed), as the potential catalytic activity of the former is inhibited by the presence of the latter.
4. Pure reed ash exhibits fusion temperatures ~260 °C higher than those of wood ash, enabling gasification of reed char at higher temperatures (thus increasing its reactivity) without creating avoidable operational problems.
5. Ash fusion temperatures for wood-reed blends may be lower than for either fuel used alone, and reach minimum values when the wood ash proportion is in the range 46–66 %. This corresponds to a (dry weight basis) blend of 83–92 % parent wood with reed. In other words, the addition of 8–17 % (by weight) of reed to wood parent fuel can be expected to lower the ash fusion temperature and, therefore, the maximum advisable gasification temperature, by ~100 °C. Therefore, particular attention must be paid to ash fusion characteristics when wood and reed are blended in such ratios.
6. Increasing the proportion of reed in the parent fuel blend above ~20 % will raise the ash fusion temperature until, for a blend containing ~40 % reed (with ~60% parent wood, dry weight basis), it will be similar to that for wood fuel alone, and higher proportions of reed will render even higher temperatures practical.
7. More generally, when reed has to be blended with other types of biomass, it is recommended that the ash fusion characteristics are first determined, then the highest temperatures that are allowable on that basis should be applied.

ACKNOWLEDGEMENTS

Deutsche Bundesstiftung Umwelt, Johan Gadolin Scholarship programme, Technische Universität München, Åbo Akademi, Brown University and European Social Fund's Doctoral Studies and Internationalisation Programme DoRa are acknowledged for the financial support and collaboration. Peter Backman, Linus Silvander, Maaris Nuutre, Raaja Aluvee, are acknowledged for a comprehensive assistance on carrying out the tests. Dr. Matthias Thommes from Quantachrome, Inc. is acknowledged for his valuable comments and discussions. This article is based on a presentation delivered at the international conference on the utilisation of emergent wetland plants "*Reed as a Renewable Resource"*, held on 14–16 February 2013 at the University of Greifswald, Germany.

REFERENCES

Arvelakis, S., Folkedahl, B., Dam-Johansen, K. & Hurley, J. (2006) Studying the melting behavior of coal, biomass, and coal/biomass ash using viscosity and heated stage XRD data. *Energy Fuels*, 20, 1329–1340.

Arvelakis, S. & Frandsen, F.J. (2007) Melting behaviour of ashes from the co-combustion of coal and straw. *Energy Fuels*, 21, 3004–3009.

Arvelakis, S., Jensen, P.A. & Dam-Johansen, K. (2004) Simultaneous thermal analysis (STA) on ash from high-alkali biomass. *Energy Fuels*, 18, 1066–1076.

Barrio, M., Gøbel, B., Risnes, H., Henriksen, U., Hustad, J.E. & Sørensen, L.H. (2001) Steam gasification of wood char and the effect of the hydrogen inhibition on the chemical kinetics. In: Bridgwater, A.V. (ed.) *Progress In Thermochemical Biomass Conversion*, Vol. 1, IEA Bioenergy, Blackwell Sciences, Oxford, 32–46.

Bar-Ziv, E. & Kantorovich, I.I. (2001) Mutual effects of porosity and reactivity in char oxidation. *Progress in Energy and Combustion Science*, 21, 667–697.

Brunauer, S., Emmett, P.H. & Teller, E. (1938) Adsorption of gases in multimolecular layers. *Journal of the American Chemical Society*, 60, 309–319.

Cetin, A., Gupta, R. & Moghtaderi, B. (2005) Effect of pyrolysis pressure and heating rate on radiata pine char structure and apparent gasification reactivity. *Fuel*, 84, 1328–1334.

Chantre, G., Rozenberg, P., Baonza, V., Macchioni, N., Le Turcq, A., Rueff, M., Petit-Conil, M. & Heois, B. (2002) Genetic selection within Douglas fir (*Pseudotsuga menziesii*) in Europe for papermaking issues. *Annals of Forest Science*, 59, 583–593.

Della Rocca, P.A., Cerrella, E.G., Bonelli, P.R. & Cukierman, A.L. (1999) Pyrolysis of hardwoods residues: on kinetics and char characterization. *Biomass and Bioenergy*, 16, 79–88.

Figueiredo, J.L. & Moulijn, J.A. (1986) *Carbon and Coal Gasification: Science and Technology*. Springer, New York, 291 pp.

Gregg, S.J. & Sing, K.S.W. (1982) *Adsorption, Surface Area and Porosity*. Academic Press, London, 303 pp.

Hansen, L.A., Frandsen, F.J., Dam-Johansen, K. & Sørensen, H.S. (1999) Quantification of fusion in ashes from solid fuel combustion. *Thermochimica Acta*, 326, 105–117.

Hupa, M. (2012) Ash-related issues in fluidized-bed combustion of biomasses: recent research highlights. *Energy Fuels*, 26, 4–14.

Ikonen, I. & Hagelberg, E. (eds.) (2007) *Read Up On Reed!* Southwest Finland Regional Environment Centre, Turku, Finland, 61 pp.

Jüntgen, H. (1983) Application of catalysts to coal gasification processes. Incentives and perspectives. *Fuel*, 62, 234–238.

Kannan, M.P. & Richards, G.N. (1990) Gasification of biomass chars in carbon dioxide: dependence of gasification rate on the indigenous metal content. *Fuel*, 69, 747–753.

Khan, A.A., Jonga, W.D., Jansens, P.J. & Spliethoff, H. (2009) Biomass combustion in fluidized bed boilers: potential problems and remedies. *Fuel Process Technology*, 90, 21–50.

Lastoskie, C., Gubbins, K.E. & Quirke, N. (1993) Pore-size distribution analysis of microporous carbons - a density-functional theory approach. *Journal of Physical Chemistry*, 97, 4786–4796.

Leofanti, G., Padovan, M., Tozzola, G. & Venturelli, B. (1998) Surface area and pore texture of catalysts. *Catalysis Today*, 41, 207–219.

Liliedahl, T. & Sjöström, K. (1997) Modelling of char-gas reaction kinetics. *Fuel*, 76, 29–37.

Link, S., Arvelakis, S., Spliethoff, H., De Waard, P. & Samoson, A. (2008) Investigation of biomasses and chars obtained from pyrolysis of different biomasses with solid-state ^{13}C and ^{23}Na nuclear magnetic resonance spectroscopy. *Energy Fuels*, 22, 3523–3530.

Livneh, T., Bar-Ziv, E., Salatino, P. & Senneca, O. (2000) Evolution of reactivity of highly porous chars from Raman microscopy. *Combustion Science and Technology*, 153, 65–82.

Ljungblom, L. (2009) The world of pellets. *Bioenergy International*, 6, 9.

Lozano-Castello, D., Cazorla-Amoros, D. & Linares-Solano, A. (2004) Usefulness of CO_2 adsorption at 273 K for the characterization of porous carbons. *Carbon*, 42, 1233–1242.

Moilanen, A. (2006) *Thermogravimetric Characterisations of Biomass and Waste for Gasification Processes*. Ph.D. Thesis, VTT Technical Research Centre of Finland, Espoo, 196 pp.

Moilanen, A. & Mühlen, H.-J. (1996) Characterization of gasification reactivity of peat char in pressurized conditions: Effect of product gas inhibition and inorganic material. *Fuel*, 75, 1279–1285.

Radović, L.R., Walker, P.L.Jr. & Jenkins, R.G. (1983) Importance of carbon active sites in the gasification of coal chars. *Fuel*, 62, 849–856.

Risnes, H., Sørensen, L.H. & Hustad, J.E. (2001) CO_2 reactivity of chars from wheat, spruce and coal. In: Bridgwater, A.V. (ed.) *Progress In Thermochemical Biomass Conversion*, Vol. 1, IEA Bioenergy, Blackwell Sciences, Oxford, 61–72.

Saidur, R., Abdelaziz, E.A., Demirbas, A., Hossain, M.S. & Mekhilef, S. (2011) A review on biomass as a fuel for boiler. *Renewable and Sustainable Energy Reviews*, 15, 2262–2289.

Sørensen, L.H., Fjellerup, J., Henriksen, U., Moilanen, A., Kurkela, E. & Winther, E. (2000) *An Evaluation of Char Reactivity and Ash Properties in Biomass Gasification. Fundamental Processes in Biomass Gasification*. ReaTech, Roskilde, Denmark, 115 pp.

Struis, R.P.W.J., Von Scala, C., Stucki, S. & Prins, R. (2002) Gasification reactivity of charcoal with

CO_2. Part I: Conversion and structural phenomena. *Chemical Engineering Science*, 57, 3581–3592.

Sutton, D., Kelleher, B. & Ross, J.R.H. (2001) Review of literature on catalysts for biomass gasification. *Fuel Processing Technology*, 73, 155–173.

Tillman, D.A., Duong, D.N.B. & Harding N.S. (2012) *Solid Fuel Blending. Principles, Practices, and Problems*. Butterworth-Heinemann, Kidlington, Oxford, 335 pp.

Van Heek, K.H. & Mühlen, H.-J. (1985) Aspects of coal properties and constitution important for gasification. *Fuel*, 64, 1405–1414.

Vamvuka, D., Pitharoulis, M., Alevizos, G., Repouskou, E. & Pentari, D. (2009) Ash effects during combustion of lignite/biomass blends in fluidized bed. *Renewable Energy*, 34, 2662–2671.

Whitty, K., Backman, R. & Hupa, M. (1998) Influence of char formation conditions on pressurized black liquor gasification rates. *Carbon*, 36, 1683–1692.

Wood, B.J. & Sancier, K.M. (1984) The mechanism of the catalytic gasification of coal char: A critical review. *Catalysis Reviews - Science and Engineering*, 26, 233–279.

Zevenhoven-Onderwater, M., Backman, R., Skrifvars, B.-J. & Hupa, M. (2001) The ash chemistry in fluidised bed gasification of biomass fuels. Part I: predicting the chemistry of melting ashes and ash–bed material interaction. *Fuel*, 80, 1489–1502.

Zanzi, R., Sjöström, K. & Björnbom, E. (1996) Rapid high-temperature pyrolysis of biomass in a free-fall reactor. *Fuel*, 75, 545–550.

Submitted 31 May 2013, revision 10 Oct 2013
Editor: Olivia Bragg

Author for correspondence:
Dr Siim Link (PhD), Department of Thermal Engineering, Tallinn University of Technology, Kopli 116, 11712, Tallinn, Estonia. Tel: +372 620 3900; Fax: +372 620 3901; E-mail: siim.link@ttu.ee